# Photovoltaic performance of an alternating cold–hot method deposited CdSe thin films

*Yaoyao Jiang[1], Yan Li[1], Danyu Wang[1], Deqing Mo[2], Fuxin Zhong[1] ✉, Yunpeng Gao[1], Yinian Zhu[1,3]*

[1]*College of Chemistry and Bioengineering, Guilin University of Technology, Guilin 541006, People's Republic of China*
[2]*College of Life and Environmental Science, Guilin University of Electronic Science and Technology, Guilin 541006, People's Republic of China*
[3]*College of Environmental Science and Engineering, Guilin University of Technology, Guilin 541006, People's Republic of China*
✉ *E-mail: zfuxin189@sina.com*

Published in Micro & Nano Letters; Received on 6th October 2016; Revised on 2nd December 2016; Accepted on 17th February 2017

Cadmium selenide (CdSe) thin films were prepared on indium tin oxide substrate by an alternating cold–hot method, in which cadmium nitrate solution was used as a cold deposition solution, while sodium selenite and potassium borohydride mixed solution was used as a hot deposition solution. The influences of the preparation conditions such as the concentration of $Cd(NO_3)_2$, the number of deposition cycle and the cycle time, on the photoelectric performance of the sample under simulated sunlight were explored. The results show that the CdSe thin film prepared under the reaction conditions of 0.06 mol/l $Cd(NO_3)_2$ at the tenth deposition cycle (30 s per cycle) reaches the highest photovoltage of 0.285 V. Under the simulated solar illumination, the open-circuit voltage and short-circuit currents are 0.419 V and 5.57 mA/cm$^2$, respectively. X-ray diffraction indicates that the strongest diffraction peak at 42.215° of the (111) crystal plane is corresponding to 15.15 nm CdSe nanocrystals. Scanning electron microscopy observation shows that the thickness of the CdSe film is about 200 nm and the size of the spherical and uniformly dispersed nanocrystals is around 50 nm.

**1. Introduction:** Owing to their unique optical and electronic properties [1–3], cadmium chalcogenides (Cd*X*, *X* = S, Se and Te) have attracted great attention in many fields [4]. Cadmium selenide (CdSe) nanoparticles are classified as an n-type II–VI semiconductor with 1.74 eV direct bandgap [5, 6]. Therefore, CdSe are used to make thin film solar cells [7, 8], photovoltaic detectors [9], biological fluorescence labelling [10] and other optoelectronic devices [11, 12]. The crystalline forms of CdSe include cubic and hexagonal structures. However, the cubic structure is unstable and converts to the hexagonal form as the annealing temperature reaches 520°C [13]. There are several methods to prepare CdSe thin films such as thermal evaporation [14–16], electrodeposition [17–19], molecular beam epitaxy [20–22], chemical bath deposit [23–25], sol–gel method [26, 27] and hydrothermal method [28–30]. Recently, chemical bath deposit method is very popular because the thickness, chemical compositions and structure of the CdSe thin films are much easier to control. Choi *et al.* [31] fabricated sandwich-type quantum dot-sensitized solar cells (QDSSCs) (CdSe/CdS/ZnO) on fluorine-doped tin oxide substrate by chemical bath deposit [32]. Here, we propose an improved chemical bath deposition of CdSe thin films by alternating use of cold and hot deposition solutions. This alternating cold–hot method utilises cold cadmium nitrate ($Cd(NO_3)_2{\cdot}4H_2O$) solution and hot sodium selenite ($Na_2SeO_3$) and potassium borohydride ($KBH_4$) mixed solution as deposition solutions. Indium tin oxide (ITO) substrate is repeatedly soaked and lifted in such cold and hot solutions in sequence to form continuous $Cd^{2+}$ and $Se^{2-}$ ion layers, i.e. CdSe nano-films are synthesised under the hot and cold temperature difference. The proposed alternating cold–hot method presents several advantages, including low cost, non-pollution, good repeatability and simple operation. The better optical and electrical performances of the CdSe thin films can be achieved by adjusting the concentration of reactants and the number of deposition cycle.

**2. Experimental results:** Analytical-grade $Na_2SeO_3$, $Cd(NO_3)_2{\cdot}4H_2O$ and $KBH_4$ were used directly without further purification. An ITO substrate with dimensions of 60 × 10 × 1 mm was ultrasonically cleaned with acetone, ethanol and deionised water for 10 min in sequence, then quickly dried in air. About 8°C cold solution A [20 ml 0.06 mol/l $Cd(NO_3)_2$] was prepared by immersing in the ice water. A colourless mixture of 10 ml 0.6 mol/l $Na_2SeO_3$ and 10 ml 0.06 mol/l $KBH_4$ was heated to 80°C and designated as the hot solution (B). The clean ITO was first vertically immersed into the solution A for 15 s and then into the solution B for 15 s to complete one deposition cycle. CdSe was deposited on the ITO as a red–brown solid. After deposition, the substrate was removed from the solutions, rinsed with deionised water and dried at room temperature. To study the effects of the cycle number, the concentration of $Cd(NO_3)_2$ and the cycle time on the properties of the CdSe thin films, three series of samples were prepared. In the first series, the properties of the films obtained under the cycles of 4, 7, 10, 14 and 20 were compared. In the second series, the effects of the $Cd(NO_3)_2$ concentrations of 0.03, 0.04, 0.06, 0.08 and 0.10 mol/l were compared. Finally, in the third series, the effects of the cycle times of 10, 20, 30, 40 and 60 s were compared.

In a typical synthesis process, oxidation–reduction can take place in a hot solution of $Na_2SeO_3$ and $KBH_4$, the forming intermediates then react with $Cd^{2+}$ to deposit CdSe on the surface of the ITO substrate. The reaction process can be simply expressed by the following equations

$$2SeO_3^{2-} + 3BH_4^- \rightarrow 2Se^{2-} + 3BO_2^- + 6H_2 \quad (1)$$

$$Cd^{2+} + Se^{2-} \rightarrow CdSe \quad (2)$$

The alternating cold–hot method promotes the facile absorption of $Cd^{2+}$ onto the ITO surface under low temperatures according to the Gibbs equation [33]. High temperatures are also highly beneficial to the reduction of the surface tension of the solution and the induction of rapid oxidation–reduction [34].

**3. Results and discussion:** Scanning electron microscopy (SEM, S-4800, Netherlands) and X-ray diffraction (XRD) with

monochromatic high-intensity Cu $K\alpha$ radiation ($\lambda = 0.15406$ nm) were applied to characterise the fabricated CdSe thin films. The photoelectrochemical properties of the films were investigated by using a conventional three-electrode system linked to an electrochemical workstation (CH Instruments, Model CHI660E). The ITO substrate containing CdSe was used as working electrode, platinum wire was used as counter electrode and calomel electrode was used as reference electrode. Photovoltage −time ($\varphi - t_{light}$) and photocurrent-voltage ($J$-$V$) measurements were carried out in 0.5 mol/l $Na_2SO_4$ solution under the dark and illuminated conditions. A solar simulator (590 W Model 9115X, Newport) with an Air Mass (AM) 1.5 spectrum distribution was used as irradiation source and calibrated against an National Renewable Energy Laboratory (NREL) reference cell to accurately simulate one full-sun intensity (100 mW/cm$^2$) [35]. Photovoltage, the photovoltaic effect of solid surface, is the result of optical electronic transitions and can be calculated through the difference between the voltages under the illumination and in the dark (3) [36, 37]. Moreover, in a common photovoltaic measurements, the series photovoltage ($U_{ph}$) can be defined as

$$U_{ph} = \varphi_{ON} - \varphi_{OFF} \tag{3}$$

$\varphi_{ON}$ is the voltage under the illumination, $\varphi_{OFF}$ is the voltage in the dark, and $t_{light}$ is the response time of the visible open-circuit potential.

The crystal structure and phase purity of the product are characterised by XRD. The XRD patterns of the deposited CdSe thin films showing a cubic zinc blende structure are illustrated in Fig. 1. Two dominant diffraction peaks are observed at $2\theta$ of 25.480° and 42.215°, one reflects the (111) plane and another reflects the (220) plane. A sharp peak at $2\theta$ of 32.480° is attributed to the selenium oxidation by oxygen in the air. According to the Debye–Scherrer equation, the average size of the nanocrystals can be calculated by the equation $D = \kappa\lambda/\beta \cos\theta$ [38] (where $D$ is the average crystallite size of the nanocrystals, $\lambda$ is the wavelength of the X-ray radiation, in this case 0.15406 nm, $\beta$ is the full-width at half-maximum (FWHM) intensity of the peak, $\theta$ is the angle at which the diffraction peak occurs and $\kappa$ is a constant with a value of 0.94 for CdSe [39]). XRD analysis reveals that each spherical particle contains several nanocrystals and the average size of the nanocrystals is 15.15 nm.

Fig. 2 shows the diffraction patterns under different deposition cycles. Four mainly diffraction peaks at 23.513°, 25.354°, 42.249° and 49.682° are corresponding to the (100) crystal faces of hexagonal CdSe (powder diffraction file database (PDF) # 19-0191) and the (111), (220) and (311) crystal faces of cubic CdSe (PDF # 08-0459). Among them, the diffraction peak of the (311) crystal face of cubic CdSe exists all the time. When the deposition cycles is four, only the diffraction peak of the (111) cubic

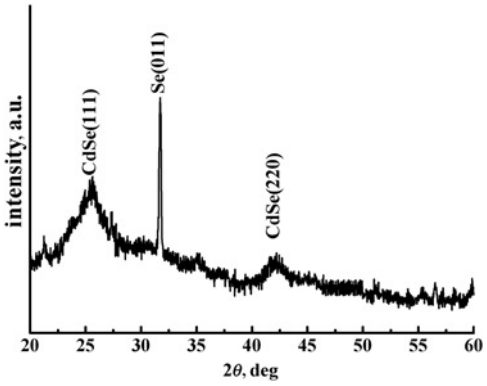


**Fig. 1** *XRD pattern of CdSe thin films*

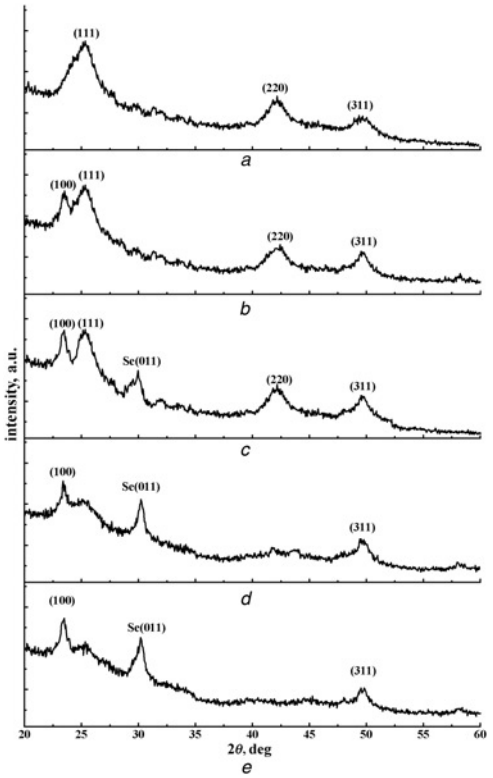


**Fig. 2** *XRD pattern of CdSe thin film [0.06 mol/l $Cd(NO_3)_2$, 30 s/cycle] under different deposition cycles*
*a* 4 Cycles
*b* 7 Cycles
*c* 10 Cycles
*d* 14 Cycles
*e* 20 Cycles

CdSe shows stronger. When the deposition cycles are up to seven, the mixed crystal of hexagonal and cubic CdSe appears. With the deposition cycles on the increase, the diffraction peak of the (100) hexagonal CdSe gradually strengthens, whereas the (111) and (220) cubic CdSe gradually weakens. When the cycles reach ten, the diffraction peak of Se crystal begins to appear. When the cycle number is between 14 and 20, the diffraction peaks of the (111) and (220) cubic CdSe disappear and the diffraction peak of the (011) crystal face of Se becomes much stronger. This indicates that with the increasing of the cycles, the deposited film becomes thicker. The longer staying time in the air, the more element Se precipitates, which leads to the impure film and promotes the growth of the (100) hexagonal CdSe and inhibits the growth of the (220) cubic CdSe. Therefore, the crystal type,

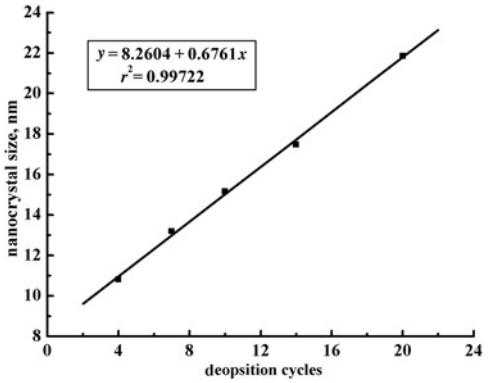


**Fig. 3** *Relational function between the number of deposition cycles and the size of CdSe nanocrystals*




doi: 10.1049/mnl.2016.0580

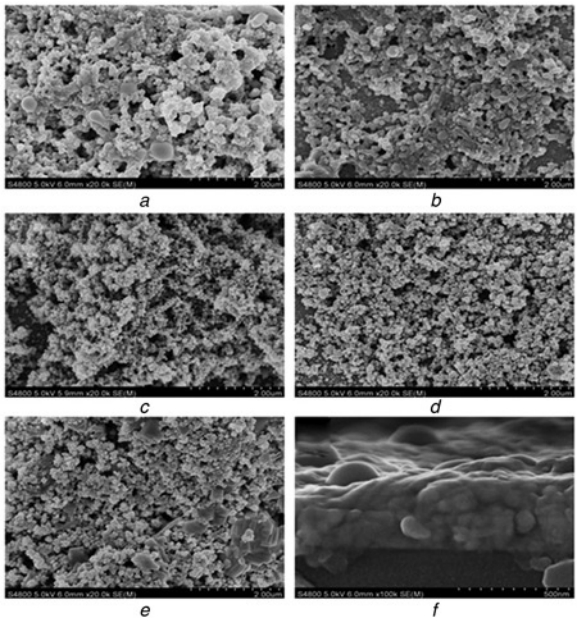


**Fig. 4** *SEM image of CdSe thin films [0.06 mol/l $Cd(NO_3)_2$, 30 s/cycle] under*
*a* 4 Cycles
*b* 7 Cycles
*c* 10 Cycles
*d* 14 Cycles
*e* 20 Cycles
*f* Thickness of the films obtained after 10 cycles

thickness and purity of the CdSe films can be controlled by changing the number of deposition cycle.

As shown in Fig. 3, according to the FWHM data of the (311) CdSe diffraction peak, the grain size and the number of deposition cycles of CdSe can be calculated by Debye–Scherrer equation [40, 41]. The average grain size of CdSe increases linearly with the increase of the cycle number.

SEM images of the CdSe thin films are shown in Figs. 4*a–f*. The size of the CdSe particles is relative uniform, but the surface of the thin films is uneven. Owing to agglomeration, the size of the CdSe particles (about 50 nm) obtained from the SEM images is larger. Fig. 4*f* shows the thickness of the films obtained after ten cycles. As the surface of the CdSe thin films is flat, the thickness of it is around 200 nm.

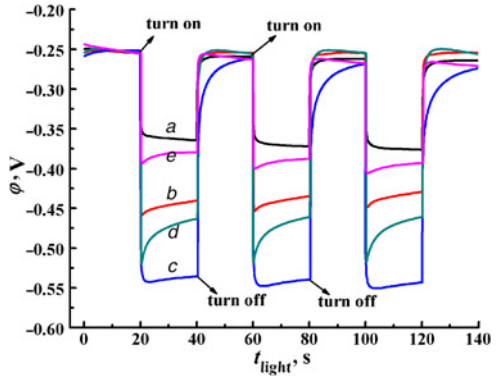


**Fig. 5** *Effect of deposition cycles on the visible open-circuit voltage of the sample [0.06 mol/l $Cd(NO_3)_2$, 30 s/cycle]*
*a* 4 Cycles
*b* 7 Cycles
*c* 10 Cycles
*d* 14 Cycles
*e* 20 Cycles

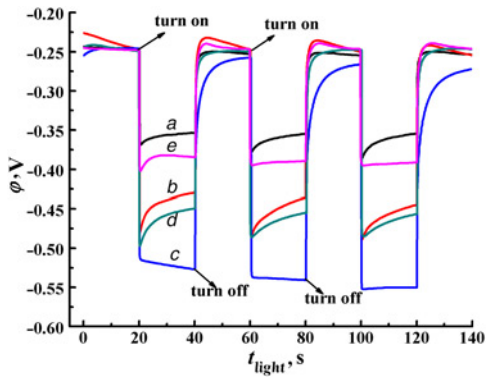


**Fig. 6** *Effect of the concentration of $Cd(NO_3)_2$ on the visible open-circuit voltage of the sample [30 s/cycle, 10 cycles]*
*a* 0.03 mol/l
*b* 0.04 mol/l
*c* 0.06 mol/l
*d* 0.08 mol/l
*e* 0.10 mol/l

Fig. 5 shows that the cycles exert a great influence on the photovoltage of the films. With increasing of the cycle number, the photovoltage of the thin films increases to a maximum value and then decline. The highest photovoltage of 0.285 V can be generated at the tenth deposition cycles. This might be explained by the effects of the thickness of the deposited CdSe thin films. When the cycles are <10, the forming layer is too thin to support a large number of photon-generated carriers. As the cycle number increases, the amount of deposited CdSe gradually increases and the number of photon-generated carriers produced per unit area is enhanced. Therefore, the photovoltage gradually increases. When the cycles exceed ten, the thin films become too thick and the resistance of the electrode increases. Consequently, the photovoltage of the films is gradually reduced.

The concentrations of $Cd(NO_3)_2$ have great effects on the morphology, corrosion and photovoltage of the sample. The open-circuit voltage response curves under the concentrations of $Cd(NO_3)_2$ 0.03, 0.04, 0.06, 0.08 and 0.10 mol/l were shown in Fig. 6. About 0.06 mol/l $Cd(NO_3)_2$ results in the highest voltage of 0.282 V. The initial availability of $Cd^{2+}$ ions on the conductive glass substrate is believed to increase rapidly with increasing concentration of $Cd(NO_3)_2$ [42]. When the ITO is inserted into a hot solution containing $Se^{2-}$, $Cd^{2+}$ reacts promptly to provide more CdSe crystal nuclei,

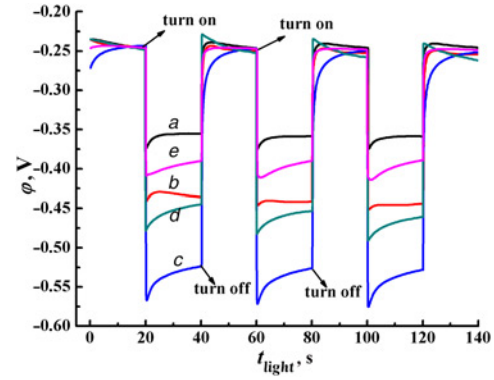


**Fig. 7** *Effect of the different cycle times on the visible open-circuit voltage of the sample [0.06 mol/l $Cd(NO_3)_2$, 10 cycles]*
*a* 10 s/cycle
*b* 20 s/cycle
*c* 30 s/cycle
*d* 40 s/cycle
*e* 50 s/cycle

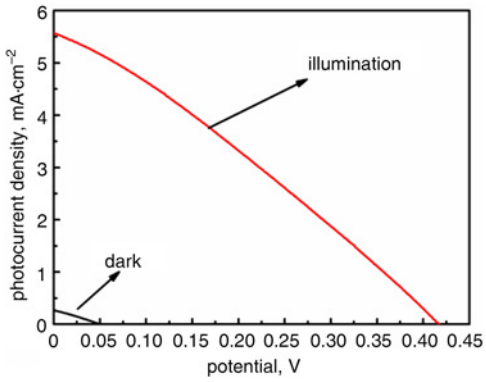


**Fig. 8** *Photocurrent- voltage (J–V) curve of the sample in the dark and under illumination*

and the surface of the ITO is nearly completely covered with these crystals. However, if the concentration of $Cd(NO_3)_2$ is excessively high under isothermal conditions, the reaction rate increases and the resulting film becomes too thick, causing uneven film surface. This is harmful to electronic transmission in the film and its photovoltage decreases.

Fig. 7 shows the influence of cycle time on the photovoltage of the films. Prolonging the cycle time causes the generated photovoltage of the thin films to initially increase to a maximum value and then decline. The highest photovoltage of 0.284 V is generated, when the cycle time is 30 s per cycle. If the dipping time of the ITO substrate in the hot solution is too short (<20 s/cycle), the reaction of $Cd^{2+}$ and $Se^{2-}$ is inadequate and a relatively low photovoltage is obtained. However, if the dipping time of the ITO substrate in the hot solution is too long (more than 30 s/cycle), the films split away off the ITO substrate and the thickness of the layer will decrease, which can also cause the photovoltage decrease.

As shown in Fig. 8, the photovoltaic responses dramatically improved under simulated 1 sun 1.5 AM solar illumination. The photovoltaic performance parameters of the *J–V* curve analysis [43] are summarised by plotting software as shown in Table 1. The photoelectric conversion efficiency ($\eta$) and fill factor (FF) [44] are important parameters to characterise the film quality and the load capacity of solar cell, respectively. As a result, the load capacity of the CdSe thin films under the illumination was significantly higher than that in the dark, and the photoelectric conversion efficiency of the CdSe thin films can reach 1.66% under the illumination. The solar cell photoelectric conversion efficiency and FF [45] were being calculated from (4) and (5) as follows

$$\eta = \frac{P_{\text{out}}}{P_{\text{in}}} = \frac{FF \times J_{\text{sc}} \times V_{\text{oc}}}{P_{\text{in}}} = \frac{J_m \times V_m}{P_{\text{in}}} \quad (4)$$

$$\text{FF} = \frac{J_m \times V_m}{J_{\text{sc}} \times V_{\text{oc}}} \quad (5)$$

where $P_{\text{out}}$ is the generated optimum output power and $P_{\text{in}}$ is the optimum input power received by the unit area of the sample under the illumination. $J_{\text{sc}}$ and $J_m$ are the short-circuit current and the optimum operating current generated by the unit area of the sample under the illumination. $V_{\text{oc}}$ is the open-circuit potential and $V_m$ is the optimum operating voltage.

**Table 1** Photovoltaic parameters of the CdSe sample in the dark and under the illumination

| | $V_{\text{oc}}$/V | $J_{\text{sc}}$, mA cm$^{-2}$ | $V_m$, V | $J_m$, mA cm$^{-2}$ | FF, % | $\eta$, % |
|---|---|---|---|---|---|---|
| dark | 0.049 | 0.24 | 0.028 | 0.14 | 34.58 | 0.04 |
| illumination | 0.419 | 5.57 | 0.267 | 4.54 | 51.88 | 1.66 |

**4. Conclusion:** A CdSe photoelectric material was successfully prepared on ITO substrate by an alternating hot–cold method. The highest photovoltage of 0.285 V was achieved under the reaction conditions of 0.06 mol/l $Cd(NO_3)_2$ at the tenth deposition cycles with 30 s per cycle. Moreover, under simulated 1 sun 1.5 AM solar illumination, $J_{\text{sc}}$, $V_{\text{oc}}$ and FF of the films are 5.57 mA cm$^{-2}$, 0.419 V and 51.88%, respectively. XRD indicates that the samples are in CdSe pure phase and the crystallinity is good. SEM shows that the thickness of the film is about 200 nm and the size of the spherical and uniformly dispersed particle is around 50 nm. This research could provide experimental and theoretical foundation for the preparation of CdSe Quantum Dots (QDs) as well as their associated Positive and Negative (PN)-type heterojunction.

**5. Acknowledgments:** The authors gratefully acknowledge the National Nature Science Foundation of China (grant no. 61264007), the Guangxi Science and Technology Development Project (GuiKeZhong grant no. 1298002-3) and Universities Science and technology research project of Guangxi (grant no. ZD2014061) for providing financial support for this project.

## 6 References

[1] Ameri M., Mesbah S., Al-Douri Y., *ET AL.*: 'First-principles calculations of structural, electronic, optical, and thermodynamic properties of CdS, CdTe and their ternary alloys $CdS_{1-x}Te_x$ $(0.0 \le x \le 1.0)$', *Acta Phys. Pol. A*, 2014, **125**, (5), pp. 1110–1117
[2] Lahewil A.S.Z., Al-Douri Y., Hashim U., *ET AL.*: 'Structural and optical investigations of cadmium sulfide nanostructures for optoelectronic applications', *Sol. Energy*, 2012, **86**, (11), pp. 3234–3240
[3] Al-Douri Y., Reshak A.H.: 'Analytical investigations of CdS nanostructures for optoelectronic applications', *Opt., Int. J. Light Electron Opt.*, 2015, **126**, (24), pp. 5109–5114
[4] Yadav A.A., Barote M.A., Masumdar E.U.: 'Studies on cadmium selenide (CdSe) thin films deposited by spray pyrolysis', *Mater. Chem. Phys.*, 2010, **121**, (1), pp. 53–57
[5] Xie Y.L.: 'Enhanced photovoltaic performance of hybrid solar cell using highly oriented CdS/CdSe-modified $TiO_2$ nanorods', *Electrochim. Acta*, 2013, **105**, pp. 137–141
[6] Zhu C., Pan X., Ye C., *ET AL.*: 'Effect of CdSe quantum dots on the performance of hybrid solar cells based on ZnO nanorod arrays', *Ceram. Int.*, 2013, **39**, (3), pp. 2975–2980
[7] Zhu D., Ye H., Zhen H., *ET AL.*: 'Improved performance in green light-emitting diodes made with CdSe-conjugated polymer composite', *Synth. Met.*, 2008, **158**, (21), pp. 879–882
[8] Wang Q., Ye F., Fang T., *ET AL.*: 'Bovine serum albumin-directed synthesis of biocompatible CdSe quantum dots and bacteria labeling', *J. Colloid Interface Sci.*, 2011, **355**, (1), pp. 9–14
[9] Zhang X.L., Wu H.F., Luo X.D., *ET AL.*: 'Research development of CdSe nano materials for solar cells', *Electr. Comput. Mater.*, 2014, **33**, (3), pp. 9–14
[10] Yin Z.G.: 'Synthesis and photoelectrochemical study on CdSe nanorod' (Hebei University of Science and Technology, Xianning, China, 2007)
[11] Pawar S.A., Devan R.S., Patil D.S., *ET AL.*: 'Improved solar cell performance of chemosynthesized cadmium selenide pebbles', *Electrochim. Acta*, 2013, **98**, pp. 244–254
[12] He X., Shen H., Pi J., *ET AL.*: 'Synthesis of $Cu_2ZnSnS_4$ films from sequentially electrodeposited Cu–Sn–Zn precursors and their structural and optical properties', *J. Mater. Sci., Mater. Electron.*, 2013, **24**, (11), pp. 4578–4584
[13] Ali M., Syed W.A.A., Zubair M., *ET AL.*: 'Physical properties of Sb-doped CdSe thin films by thermal evaporation method', *Appl. Surf. Sci.*, 2013, **284**, pp. 482–488
[14] Shyju T.S., Anandhi S., Indirajith R., *ET AL.*: 'Solvothermal synthesis, deposition and characterization of cadmium selenide (CdSe) thin films by thermal evaporation technique', *J. Cryst. Growth*, 2011, **337**, (1), pp. 38–45
[15] Patel K.D., Jani M.S., Pathak V.M., *ET AL.*: 'Deposition of CdSe thin films by thermal evaporation and their structural and optical properties', *Chalcogenide Lett.*, 2009, **6**, (6), pp. 279–286




doi: 10.1049/mnl.2016.0580

[16] Kois J., Gurevits J., Bereznev S., *ET AL.*: 'CdSe nanofiber and nanohorn structures on ITO substrates fabricated by electrochemical deposition', *Appl. Surf. Sci.*, 2013, **283**, pp. 982–985
[17] Li J., Ma T., Wei M., *ET AL.*: 'The $Cu_2ZnSnSe_4$ thin films solar cells synthesized by electrodeposition route', *Appl. Surf. Sci.*, 2012, **258**, (17), pp. 6261–6265
[18] Avellaneda D., Nair M.T.S., Nair P.K.: 'Polymorphic tin sulfide thin films of zinc blende and orthorhombic structures by chemical deposition', *J. Electrochem. Soc.*, 2008, **155**, (7), pp. D517–D525
[19] Wang J.S., Tsai Y.H., Wang H.H., *ET AL.*: 'Enhanced growth of highly lattice-mismatched CdSe on GaAs substrates by molecular beam epitaxy', *Appl. Surf. Sci.*, 2013, **270**, pp. 751–754
[20] Sorokin S.V., Gronin S.V., Sedova I.V., *ET AL.*: 'Molecular beam epitaxy of ZnSSe/CdSe short-period superlattices for III–V/II–VI multijunction solar cells', *Semiconductors*, 2015, **49**, (8), pp. 1000–1006
[21] Gronin S.V., Sorokin S.V., Kazanov D.R., *ET AL.*: 'CdSe/ZnCdSe quantum dot heterostructures for yellow spectral range grown on GaAs substrates by molecular beam epitaxy', *Acta Phys. Pol. A*, 2014, **126**, (5), pp. 1096–1099
[22] Deshpande M.P., Garg N., Bhatt S.V., *ET AL.*: 'Characterization of CdSe thin films deposited by chemical bath solutions containing triethanolamine', *Mater. Sci. Semicond. Process.*, 2013, **16**, (3), pp. 915–922
[23] Gao C., Shen H., Sun L.: 'Preparation and properties of zinc blende and orthorhombic SnS films by chemical bath deposition', *Appl. Surf. Sci.*, 2011, **257**, (15), pp. 6750–6755
[24] Ibraheam A.S., Al-Douri Y., Azman A.H.: 'Characterization and analysis of wheat-like CdS nanostructures under temperature effect for solar cells applications', *Opt., Int. J. Light Electron Opt.*, 2016, **127**, (20), pp. 8907–8915
[25] Dhanam M., Prabhu R.R., Manoj P.K.: 'Investigations on chemical bath deposited cadmium selenide thin films', *Mater. Chem. Phys.*, 2008, **107**, (2), pp. 289–296
[26] Elisa M., Vasiliu I.C., Feraru I.D., *ET AL.*: 'CdSe/ZnS-doped silicophosphate films prepared by sol–gel method', *J. Sol-Gel Sci. Technol.*, 2015, **73**, (3), pp. 660–665
[27] Gaeeni M.R., Tohidian M., Majles-Ara M.: 'Green synthesis of CdSe colloidal nanocrystals with strong green emission by the sol–gel method', *Ind. Eng. Chem. Res.*, 2014, **53**, (18), pp. 7598–7603
[28] Nagaraju G., Chandrappa G.T.: 'Surfactant assisted hydrothermal synthesis of CdSe nanostructural materials', *J. Mater. Sci. Technol.*, 2012, **28**, (6), pp. 495–499
[29] Ghosh T., Ullah K., Nikam V., *ET AL.*: 'The characteristic study and sonocatalytic performance of CdSe–graphene as catalyst in the degradation of azo dyes in aqueous solution under dark conditions', *Ultrason. Sonochem.*, 2013, **20**, (2), pp. 768–776
[30] Sobhani A., Salavati-Niasari M.: 'Synthesis and characterization of CdSe nanostructures by using a new selenium source: effect of hydrothermal preparation conditions', *Mater. Res. Bull.*, 2014, **53**, pp. 7–14
[31] Choi Y., Seol M., Kim W., *ET AL.*: 'Chemical bath deposition of stoichiometric CdSe quantum dots for efficient quantum-dot-sensitized solar cell application', *J. Phys. Chem. C*, 2014, **118**, (11), pp. 5664–5670
[32] Ghosh T., Lee J.H., Meng Z.D., *ET AL.*: 'Graphene oxide based CdSe photocatalysts: synthesis, characterization and comparative photocatalytic efficiency of rhodamine B and industrial dye', *Mater. Res. Bull.*, 2013, **48**, (3), pp. 1268–1274
[33] Rouquerol J., Rouquerol F., Llewellyn P., *ET AL.*: 'Adsorption by powders and porous solids: principles, methodology and applications' (Academic Press, Salt Lake, America, 2013)
[34] Zhou R., Guo W., Yu R., *ET AL.*: 'Highly flexible, conductive and catalytic Pt networks as transparent counter electrodes for wearable dye-sensitized solar cells', *J. Mater. Chem. A*, 2015, **3**, (45), pp. 23028–23034
[35] He L.: 'Preparation and characterization of semiconductor photoelectrode and its photoelectrochemical properties' (Tianjin University, Tianjin, China, 2007)
[36] Marandi M., Amrollahi R., Taghavinia N.: 'Highly formed luminescent oxygen trap states in thermochemically prepared CdS nanocrystals and improvement of the luminescence property', *Synth. React. Inorg. Metal-Org Nano-Metal Chem.*, 2016, **46**, (3), pp. 327–333
[37] Cohen M., Chelikowsky J.R.: 'Electronic structure and optical properties of semiconductors' (Springer Science & Business Media, Berlin/Heidelberg, Germany, 2012)
[38] Holzwarth U., Gibson N.: 'The Scherrer equation versus the 'Debye–Scherrer equation'', *Nat. Nanotechnol.*, 2011, **6**, (9), p. 534
[39] Song X., Wang M., Shi Y., *ET AL.*: 'In situ hydrothermal growth of CdSe (S) nanocrystals on mesoporous $TiO_2$ films for quantum dot-sensitized solar cells', *Electrochim. Acta*, 2012, **81**, pp. 260–267
[40] Al-Douri Y., Waheb J.H., Ameri M., *ET AL.*: 'Morphology, analysis and properties studies of CdS nanostructures under thiourea concentration effect for photovoltaic applications', *Int. J. Electrochem. Sci.*, 2013, **8**, pp. 10688–10696
[41] Al-Douri Y., Khasawneh Q., Kiwan S., *ET AL.*: 'Structural and optical insights to enhance solar cell performance of CdS nanostructures', *Energy Convers. Manage.*, 2014, **82**, pp. 238–243
[42] Lu Y.J., Liang S., Chen M., *ET AL.*: 'Preparation of nano-crystal $Cu_2S$ films by chemical bath deposition and its optical properties', *J. Funct. Mater.*, 2008, **39**, p. 1894
[43] Al-Douri Y., Ameri M., Bouhemadou A., *ET AL.*: 'Annealing temperature effect on structural, optical, morphological and electrical properties of CdS/Si (100) nanostructures', *Microsyst. Technol.*, 2016, **22**, (10), pp. 2539–2541
[44] Skoplaki E., Palyvos J.A.: 'On the temperature dependence of photovoltaic module electrical performance: a review of efficiency/power correlations', *Sol. Energy*, 2009, **83**, (5), pp. 614–624
[45] Qi B., Wang J.: 'Fill factor in organic solar cells', *Phys. Chem. Chem. Phys.*, 2013, **15**, (23), pp. 8972–8982